

Study on Traffic Current of Lane Reduction Bottleneck under Open Boundary Condition

Zhipeng Li, Run Zhang, Shangzhi Xu and Yeqing Qian*

School of Electronics and Information Engineering, Tongji University, Shanghai 201804, China

Received: 30 May 2014, Revised: 28 Aug. 2014, Accepted: 30 Aug. 2014

Published online: 1 Mar. 2015

Abstract: In this paper, traffic current of the lane reduction bottleneck for two-lane road merging into single-lane road under open boundary condition is investigated numerically for different upstream arrival rates and downstream departure rates. We find that traffic current at the bottleneck will reach its capacity when the upstream arrival rate exceeds a critical value with a free downstream traffic flow, while the current decreases with the decrease of the downstream departure rate when the downstream departure rate is less than the capacity of the bottleneck. Two representative cases, which are downstream departure rates being less than and greater than the capacity of the bottleneck, are selected to simulate the traffic flow at the lane reduction bottleneck, and investigate the dependence of the traffic current on safety distance, length and maximum speed of slow down section for different downstream departure rates. Some practical suggestions are proposed based on the results of our investigations.

Keywords: lane reduction bottleneck, optimal velocity model, open boundary condition, saturated current.

1. Introduction

Transportation has become one of the most concern issues in our daily life because the rapid development of modern society relies on the mobility of staff severely. With the saturation of car ownership over time, the serious congestion problems and air pollution have brought heavy economic losses for all the major large and medium-sized cities every year. In the urban road network, the traffic bottleneck formed due to various reasons, has become a key point and difficulty to deal with in daily urban traffic management for its complexity during rush hour. Many traffic jams derived from the upstream and downstream traffic bottleneck on certain major thoroughfares and even on secondary main roads in city. Then many scholars with different background devoted themselves into the study of traffic bottlenecks in urban traffic network in recent years, and have made remarkable achievements.

Generally, combining computer simulation technology, special occasion simulation with traffic flow model has become the most favorable methods to explore intrinsic and inherent operation law in urban transportation system. Thus, a lot of more actual traffic flow models have been proposed to be embedded into a variety of software products for traffic flow simulation. From the research perspec-

tive, there are essentially two different types of approaches to studying traffic modeling, namely, macroscopic and microscopic modeling. As one of the latter models, the car following model in traffic flow has been theoretically studied for 50 years nearly since the earliest car following model proposed by Pipes in 1953 [1]. Its basic idea is based on a simple subjective perception, which can be described as follows: a vehicle is slower than its following vehicle, then accelerating, otherwise, then decelerating. Pipes's model belongs to the easiest and the most basic car following model, which to some extent reveals inner rules in traffic flow. Later, in 1995 Bando et al. [2] proposed the optimal velocity model (OVM), the idea of this kind of car-following model is that a driver adjusts his vehicle velocity to approach the optimal velocity determined by the observed headway. The OVM model has been studied extensively in last decades and many extended versions have been developed for its good performance in simulating the practical characteristics of traffic flow. Moreover, many important traffic characteristics have been described and some important results have been obtained by use of a variety of traffic flow microscopic models [3,4,5,6,7,8,9,10,11,12,13,14,15,16,17,18,19,20,21,22,23,24,25,26,27,28,29].

* Corresponding author e-mail: qianyeqing@tongji.edu.cn

In urban traffic, lane reduction bottleneck is one of the most common traffic bottlenecks, and one culprit leading to network congestion. The vehicles congestion and squeeze at the merging point caused by lane reduction bottleneck always bring about a bad and severe situation that the traffic current is difficult to get anywhere near its corresponding capacity at bottleneck. It is important for transport regulatory to carry out research in this area, and obtain its inherent rules of internal evolution. Applying an optimal velocity model, Zhang [30] studied traffic bottleneck characteristics at the lane reduction bottleneck of two-lane road merging into single-lane road. Some important conclusions about the traffic current and the velocity distributions in the road system have been obtained with finding that the headway and velocity discontinuously vary with the different lane. However, their work is only limited to the case under the periodic boundary condition, which is not correspondence with the real traffic characteristics somewhere. Some other researchers have investigated the traffic jams with a blockage induced by an accident car [31, 32].

As we all know, the actual traffic flow condition is under the open boundary condition, where two separate variables near the lane reduction bottleneck, which are upstream arrival rate and downstream departure rate, are independent with each other. We wonder how the traffic current at bottleneck changes with increasing the upstream arrival rate under the open boundary condition, and whether the phenomenon that the headway and velocity of the right lane being always greater than that of the left lane in slowdown section under periodic boundary condition will also appear in the case under the open boundary condition or not. It is still unknown that whether the traffic current is closely related to the safety distance, the maximum speed and the length of slowdown section, when the current at the lane reduction bottleneck saturates. Besides, we want to know how these parameters affect the traffic current at bottleneck. Here we are concentrated on these topics.

In this paper, we investigate the traffic current of lane reduction bottleneck of two-lane road merging into single-lane road under open boundary condition by using a car following model of simulation. We study the relation between the traffic current at the bottlenecks and upstream arrival rate, and the relation between the capacity of bottleneck and the downstream departure rate by numerical simulations. The distribution of vehicles in velocity and headway at the lane reduction bottleneck has been simulated with different downstream departure rates. Moreover, the dependence of the traffic current on safety distance, length and maximum speed of slow down section for different downstream departure rates.

This paper is organized as follows: In Section 2, the modeling of simulation has been proposed for the lane reduction bottleneck of two-lane road merging into single-lane road. In Section 3, the numerical simulations are performed with the asymmetric lane changing rules to study the traffic current of the lane reduction bottleneck for dif-

ferent upstream arrival rates and downstream departure rates. Section 4 is devoted to the conclusion.

2. Modeling of lane reduction bottleneck

We study the lane reduction bottleneck under the open condition. Fig.1 shows the schematic illustration of the traffic bottleneck of two-lane road merging into single-lane road under the open condition. The whole road system is divided into three sections: section A, section B and section C. The section C is a normal single-lane section, called departure section, in which the right lane is not available. The velocity of the leading vehicle in the section C is controlled by the departure rate which reflects the downstream traffic flow states. The section B is a normal slowdown section with its lower maximal velocity allowed, which is near the merging point M and is seriously influenced by the section C. the section A is a normal two-lane section, called the arrival section, which is far away from the merging point M and is not influenced by the section C. The number of vehicles entering the arrival section is different with the varied arrival rates reflecting the upstream traffic states, while the vehicles depart the section C according to the preset departure rate. Besides, the parameters in all three sections are represented as follows: the lengths of the section A, B and C are L_A, L_B and L_C respectively. Besides, maximal velocity of vehicles in the sections A and C are set as v_{max}^{AC} , which is different from the maximal velocity of vehicles v_{max}^B in the section B.

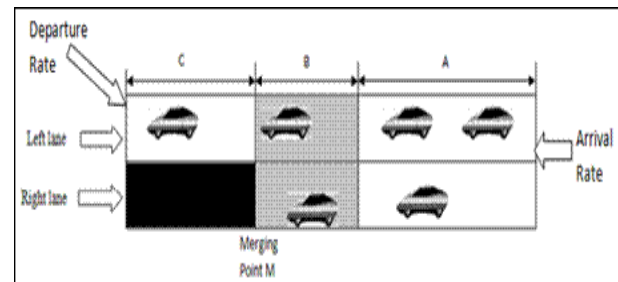


Figure 1 Schematic illustration of the road (the road is divided into three sections: section A, section B, and section C. In the section A, the symmetric lane changing rules are used, in the section B (illustrated by gray color), special lane changing rules are adopted and it is a slowdown section; in the section C, only the left lane is available, right lane illustrated by black color is closed).

The evolution of traffic flow at the lane reduction bottleneck is strictly linked to the entrance current in the left end of the section A, the sum of the vehicles entering the downstream from the section C per unit time and the vehicular movements in all three sections. Under the open

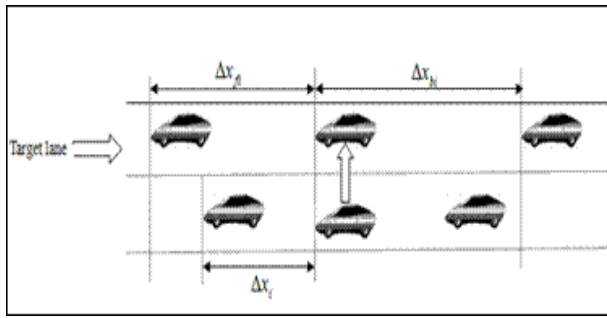


Figure 2 Schematic illustration of lane changing behavior under the two-lane road case, where the incoming vehicle on one lane enters into the middle position between two adjacent vehicles on the other lane.

boundary condition, we set up that the entrance current depends on the arrival rate, and the departure rate determines the velocity at the exit. Then the number of vehicles, the velocities and the current are influenced by different arrival rate and departure rate obviously. The vehicular movements can be separated into two stages: one is the sideways movement (lane changing movement) and the other is the forward movement as shown in Fig. 2.

The optimal velocity model is applied to the forward movement, which is one of the most classical car following models. The OVM is based on the assumption that the acceleration of the vehicle at time is determined by the difference between the actual velocity $v_n(t)$ and an optimal velocity $V(\Delta x_n(t))$:

$$\frac{dv_i(t)}{dt} = a[V(\Delta x_i(t)) - v_n(t)] \tag{1}$$

where a is the sensitivity coefficient representing the drivers reaction time. The parameter $\Delta x_i(t) = x_{i-1}(t) - x_i(t)$ is the headway between the $(i)th$ vehicle and the $(i - 1)th$ vehicle at time t .

Universally, the optimal velocity function is a monotonically increasing function, which means that its function value is proportional to the independent variable $\Delta x_i(t)$. And the function value has its upper bound (maximal velocity).

As vehicles move in sections A and C (the normal sections), the optimal velocity function is suggested by Zhang et.a [30] as follows,

$$V(\Delta x_i) = \frac{v_{max}^{AC}}{2} [\tanh(\Delta x_i - x_{safe}) + \tanh(x_{safe})] \tag{2}$$

where v_{max}^{AC} is the maximal velocity of vehicles in the sections A and C, and x_{safe} is the safety distance.

The vehicles move with the forced speed as the section B is a slowdown section with its lower speed limit $v_{B,max}$. Vehicles apply the accustomed optimal velocity function

with speed limit v_{max}^B , when entering into the slowdown section.

$$V(\Delta x_i) = \frac{v_{max}^B}{2} [\tanh(\Delta x_i - x_{safe}) + \tanh(x_{safe})] \tag{3}$$

where v_{max}^B is the maximal velocity of vehicles in the sections B, and according to the proposing of Zhang et.al [30], it can be obtained by the following equation:

$$v_{max}^B = \min(v_{B,max}, v_{max}^{AC}) \tag{4}$$

where the Eq. 4 indicates that the maximal velocity v_{max}^B in section B should be taken from the minimum value between the speed limit $v_{B,max}$ and the maximal velocity of vehicles v_{max}^{AC} in the normal sections A and C.

Generally, the sideways movement shall have obvious influence on the traffic bottleneck characteristics such as the location distribution of vehicles on the road, and the current of the traffic flow. Whats more, lane changing movement is common in two-lane road system both in normal section A and slowdown section B. However, the different rules of the lane changing is applied in the normal section A and the slowdown section B.

Section A, which is the arrival section for vehicles from upstream, is a normal two-lane section and is hardly influenced by the reduction of lanes for it is far away from the merging point M. Then the following symmetric rule of lane changing for the vehicles is suggested by Zhang et.al [30] for section A:

$$\Delta x_i < 2x_{safe} \text{ for the incentive criterion,} \tag{5}$$

$$\Delta x_{fi} > 2\Delta x_i \text{ and } \Delta x_{bi} > x_{safe} \text{ for the security criterion,} \tag{6}$$

$$rand() \leq p_A \text{ for the probability of changing lane,} \tag{7}$$

where Δx_{fi} is the headway between the vehicle i and the preceding vehicle on the target lane, and Δx_{bi} is the headway between the vehicle i and the rear vehicle in the target lane. The incentive criterion and the security criterion are needed for a vehicle to change its lane, and the probability is p_A .

As a slowdown section, the section B has different lane changing rules from the normal section A. Section B is seriously influenced by the section C for the reason that two-lane road merging into single-lane road at the merging point M, which connects the section B and the section C. Then vehicles tend to move to run on the left lane in the section B when they approach the merging point M, which means that the lane changing of vehicles from right lane to left lane is easier than that in opposite direction. These phenomena are consistent with the asymmetric lane changing rules in the section B. We adopt different lane changing rules for the vehicles on either the left lane or the right lane in the section B. The vehicles on the left lane are forced to change to right lane when its headway is satisfied

for the incentive criterion. Besides, the rules for vehicles on the left lane have to insure that all vehicles conducting lane-changing behavior are satisfied with the security criterion. The following rules of lane changing are proposed by Zhang et.al [30] for the vehicles on the left lane in the section B:

$$\Delta x_i < \frac{1}{2}x_{safe} \quad \text{for the incentive criterion,} \quad (8)$$

$$\Delta x_{fi} > 2x_{safe} \text{ and } \Delta x_{bi} > x_{safe} \quad \text{for the security criterion,} \quad (9)$$

$$rand() \leq p_B \quad \text{for the probability of changing lane,} \quad (10)$$

where $p_B \leq 0.2$ in this paper.

For the vehicles on the right lane of the section B, the lane changing rules are different because it ends at the position of the merging point M, The lane changing movement from right lane to left lane in the section B is divided into two cases, which are induced lane changing and active lane changing. On one hand, vehicles on the right lane in the section B are induced to change to the left lane which has more interspaces at the position. This movement is called induced lane changing movement. On the other hand, though smaller headway on the left lane actively the vehicle changes its lane from right lane to left lane in the section B because the right lane is expected to end at the merging point M, which is called the active lane changing movement. The asymmetric lane changing rules are mainly described in the the active lane changing movement in the section B. Then two cases of the lane changing rules for vehicles on the right lane in the section B are proposed by Zhang et.al [30] as below:

$$(1) \Delta x_i \leq \Delta x_{fi} \quad \text{for the incentive criterion,} \quad (11)$$

$$\Delta x_{bi} > \frac{1}{2}x_{safe} \quad \text{for the security criterion;} \quad (12)$$

$$(2) \Delta x_i > \Delta x_{fi}, \Delta x_{fi} > \frac{1}{2}x_{safe} \text{ and } \Delta x_i - \Delta x_{fi} < \frac{1}{2}x_{safe} \quad \text{for the incentive criterion,} \quad (13)$$

$$\Delta x_{bi} > \frac{1}{2}x_{safe} \quad \text{for the security criterion,} \quad (14)$$

$$rand() \leq 1 - p_B \quad \text{for the probability of changing lane,} \quad (15)$$

The asymmetric lane changing rules in the section B show that the vehicles in the left lane are not willing to change to the right lane and the vehicles in the right lane tend to change to the left lane, which is consistent with the real observations in traffic fields.

Probably, there are some serious lane squeezing behaviors near the merging point M as the vehicles on the

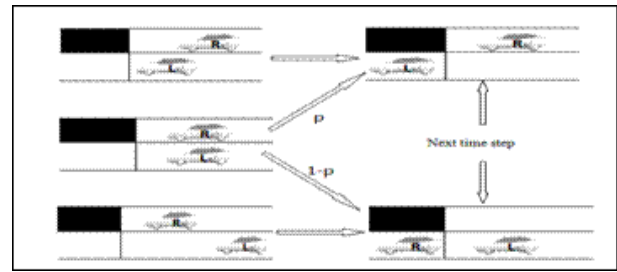


Figure 3 Schematic illustration of the lane squeezing at the merging point M.

left and right lanes of section B are approaching the merging location. What the leading vehicles on the left and right lanes scramble the possibility access to the section C brings about the lane squeezing behaviors. Moreover, the lane squeezing behaviors are also different with the different location distribution for the left leading vehicle and the right leading vehicle near the merging point. According to the different distribution of the two leading vehicles, Zhang et.al [30] suggests that the lane squeezing rules should be divided into three cases:

$$(1) x_{\text{leading}}^R - x_{\text{leading}}^L \leq 0, \quad G = 1; \quad (16)$$

$$(2) 0 < x_{\text{leading}}^R - x_{\text{leading}}^L \leq \frac{1}{2}x_{safe}, \quad G = \begin{cases} 1, & rand() \leq p_1 \\ -1 & rand() \leq 1 - p_1 \end{cases} \quad (17)$$

$$x_{\text{leading}}^R - x_{\text{leading}}^L > \frac{1}{2}x_{safe}, \quad G = -1 \quad (18)$$

where $x_{\text{leading}}^L(x_{\text{leading}}^R)$ represents the position of the leading vehicle in the left (right) lane of the section B. And $G = 1$ represents the case that the leading vehicle of the left lane enters the section C, $G = -1$ represents the case that the right leading vehicle scramble the opportunity access to the section C, and $p_1 \geq 0.75$. The parameter $p_1 \geq 0.75$ is important and influenced by all kinds of factors. We will give its approximate interval here according to the actual traffic condition.

3. Simulation results and discussion

We perform computer simulations for the lane reduction bottleneck under the open boundary condition, which is different from the periodic boundary condition conducted by Zhang et al. [30]. In this paper, we are focus on two important parameters: the upstream arrival rate at the left end of the section A (Ra, for short), and the downstream departure rate at the right end of the section C (Rd, for short). The upstream arrival rate determines the number of

vehicles arriving at the left end of section A on both lanes from upstream within a unit time while the departure rate determines the velocity of the first vehicle departing from section C respectively. The Ra and Rd essentially represent the traffic current for upstream and downstream of the bottleneck. According to the basic diagram of current against density from the OVM model as shown in Fig.4, a value of traffic current corresponds to two values in the density dimension except for the maximum current, which divides the whole plot into two parts. The left part is the climbing phase of traffic current, which nicely illustrates the increasing process of the upstream traffic current of the lane reduction bottleneck. Thus, the values of Ra in this article refer to values in the left side of Fig.4 in case there is no special instruction. Likewise, our article considers the effect of the increasing downstream traffic density on the current of the bottleneck, which corresponds to the right side of the plot. The values of Rd fall into the right part if no special instruction is provided.

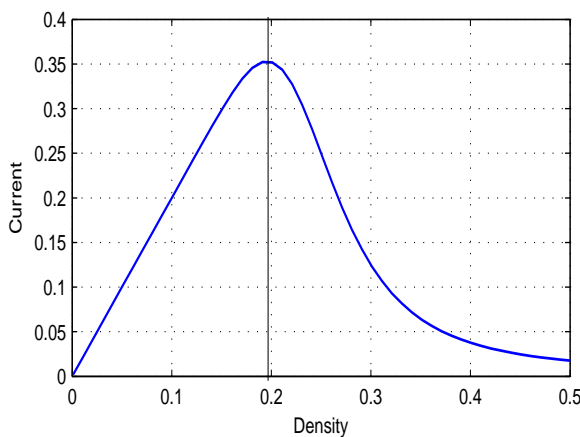


Figure 4 Diagram of traffic current against the entrance density

We study the lane reduction bottleneck under open boundary condition by using a car following model. Initially, we put the all vehicles in the sections A and B with the same headway $\Delta x_{ini}(Ra = 1/(\Delta x_{ini} * V(\Delta x_{ini}))$ and all vehicles in the sections A and B move with the same speed $v_{ini}(v_{ini} = V(\Delta x_{ini}))$. Meanwhile, the vehicles in the section C are positioned with the same headway $\Delta x_{ini}^C(Rd = 1/(\Delta x_{ini}^C * V(\Delta x_{ini}^C)))$ and all vehicles in section C move with the same speed $v_{ini}^C(v_{ini}^C = V(\Delta x_{ini}^C))$. Besides, the length of road is chosen as follows: $L = L_A + L_B + L_C, L_A = 1000m, L_B = 200m$ and $L_C = 600m$ unless otherwise stated. We choose the probabilities of lane changing and lane squeezing as follows: $p_A = 0.7, p_B = 0.2, p_1 = 0.75, p_2 = 0.9$ and $p_3 = 0.5$. Furthermore, we set the initial parameters with the sensitivity $a = 3.0$, the maximal velocity in the sections A and C

$v_{max}^{AC} = 2.0$, the speed limit in the section B $v_{B,max} = 1.2$, and the safety distance $x_{safe} = 4$. Finally, we carry out the simulations with optimal velocity model by using the fourth-order Runge-Kutta method, where the time interval is $\Delta t = 1/128$.

First, we simulate the relationship between the upstream arrival rate (Ra) and traffic current at the lane reduction bottleneck. We carry out simulation by varying the upstream arrival rates at the left side of the section A and setting the downstream traffic flow as the free flow (all vehicles in the section C move with the maximal velocity) with other initial conditions unchanged. Then the headway and velocity of all vehicles in the section A and B are changed constantly with the increase of the upstream arrival rate Ra, while the headway and velocity of all vehicles in the section C are settled with unchanged downstream departure rate Rd. Fig. 5 shows the relation between the traffic current at lane reduction bottleneck and the upstream arrival rate Ra. The plot is obtained by recording the number of the vehicle passing the lane reduction bottleneck during the 9900 – 10000 s for different upstream arrival rates Ra. From this figure, one can observe that the current at the bottleneck increases with the increase of the Ra when the upstream arrival rate Ra is less than a critical value 0.13 (vehicles/s), and the current saturates with keeping a constant (0.27) when the arrival rate is greater than the critical value. According to the concept of capacity, the constant is the capacity of the lane reduction bottleneck, and this phenomenon of the current remaining the same corresponds to the field observation at common lane reduction bottleneck in real traffic system. Namely, the capacity remains changeless with the increasing of the upstream arrival rate Ra after the traffic current of the lane reduction bottleneck saturating. It can be concluded that the capacity of the lane reduction bottleneck is not influenced by the upstream arrival rate when the downstream traffic flow is in the situation of low-traffic.

We simulate the relationship between the downstream departure rate and traffic current at the lane reduction bottleneck. We consider the case in which the upstream arrival rate (Ra) is great enough to make the current of the lane reduction bottleneck reach its capacity ($Ra > 0.13$). We assume that initially all vehicles in the section C are positioned with a same headway, and move with a same velocity determined by the downstream departure rate, which reflects the operational state of the downstream traffic flow. Similarly, the relationship between downstream departure rate and the headway of vehicles in the section C can be expressed by the Eq. 19.

$$Rd = 1/(\Delta x_{ini}^C * V(\Delta x_{ini}^C)) \tag{19}$$

Fig.6 gives the relationship between the traffic current at lane reduction bottleneck and the downstream departure rate Rd. From this figure, one can observe that the traffic current at the lane reduction bottleneck keeps its capacity (0.27) when the downstream departure rate $Rd \geq 0.27$. It means that the saturated current of the lane reduction

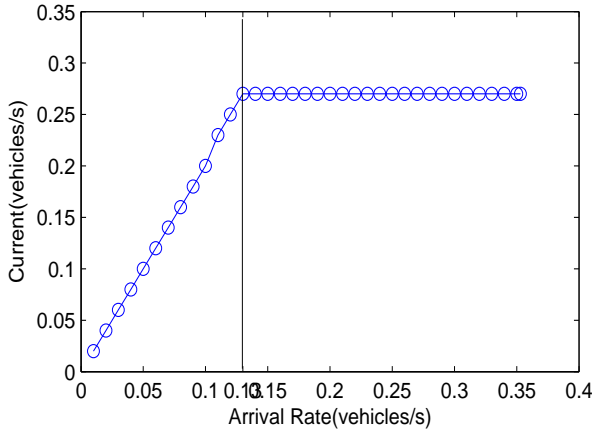


Figure 5 Relation between the traffic current at lane reduction bottleneck and the upstream arrival rate Ra.

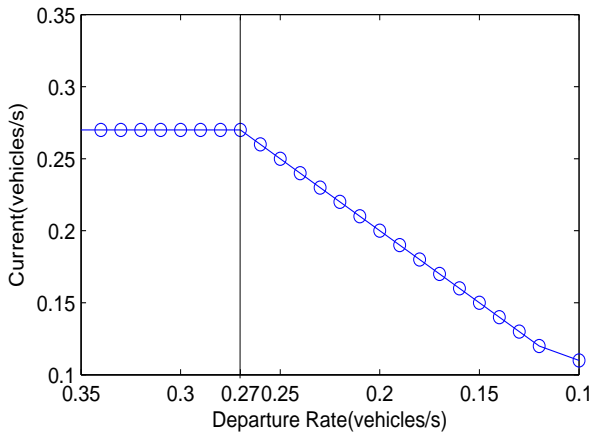


Figure 6 Relationship between the traffic current at lane reduction bottleneck and the downstream departure rate Rd.

bottleneck is not affected by the downstream department rate Rd when the number of vehicle passing the bottleneck per unit time is less than or equal to the number of vehicle departing from the section C in a unit time with the time evolution. On the other hand, the traffic current at the lane reduction bottleneck decreases with the decreasing of the downstream department rate when the downstream department rate Rd less than 0.27. The angle of decreasing in Fig.6 is approximately 45 degrees, which means in this case the number of vehicle passing the bottleneck per unit time is equal to the number of vehicle departing from the section C in a unit time with the time evolution. That is to say, the traffic current of the lane reduction bottleneck cannot saturate and is limited by the downstream traffic flow

when the downstream department rate Rd less than the capacity of the bottleneck. This is because a queue will be formed and will move left across the merging point M in Fig.1 along with the time evolution. All in all, it can be concluded that the traffic current at bottleneck can reach its capacity when the downstream departure rate is higher than the capacity of the lane reduction bottleneck. However, the traffic current of the bottleneck is also limited by the downstream traffic situation when the downstream departure rate Rd is lower than its capacity.

In order to research the internal evolution of the traffic flow at the lane reduction bottleneck in detail, two cases with two representative downstream departure rates are selected to simulate the vehicle flow when the upstream arrival rate (Ra) is great enough to make the current of the lane reduction bottleneck reach its capacity ($Ra > 0.13$). One is the case for the downstream departure rate Rd= 0.35 (Case 1), which corresponds to the case that the downstream department rate Rd being greater than 0.27(the capacity of the bottleneck), the other is the case for the downstream department rate Rd=0.12 (Case 2), which corresponds to the case that Rd being less than 0.27.

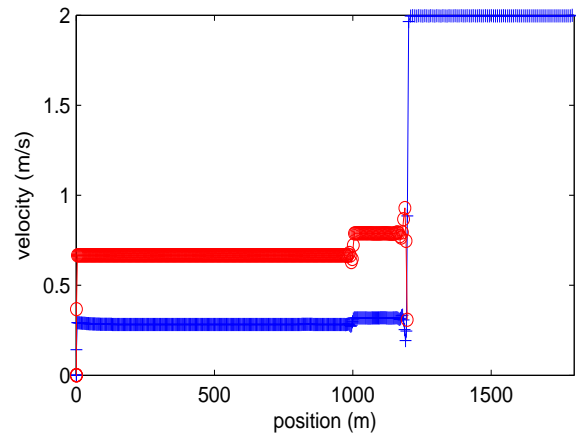


Figure 7 Snapshot of velocity against position on the whole road at the downstream departure rates Rd=0.35(vehicles/s). The red line with open circles and blue line with plus signs represent the velocity profiles of the right and left lanes respectively.

Firstly, we simulate the traffic flow for Case 1 in which the downstream department rate Rd is greater than the capacity of the lane reduction bottleneck. The distributions of headway and velocity of vehicles in the road system are obtained at sufficiently large time for the downstream department rate Rd=0.35 as shown in Figs. 7 and 8, where the upstream arrival rate Ra=0.35. From these figures, one can see that all vehicles in the section C travel with their maximum speeds 2.0m/s except the leading car which is consistent with the traffic situation of the downstream traf-

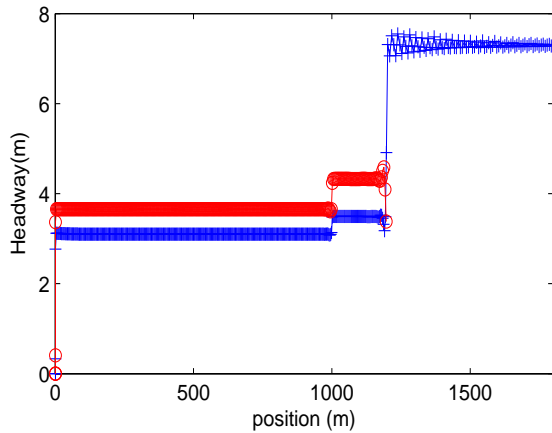


Figure 8 Snapshot of headway against position on the whole road at the downstream departure rates 0.35(vehicles/s), where the red line with open circles and blue line with plus signs represent the headway profiles of the right and left lines respectively.

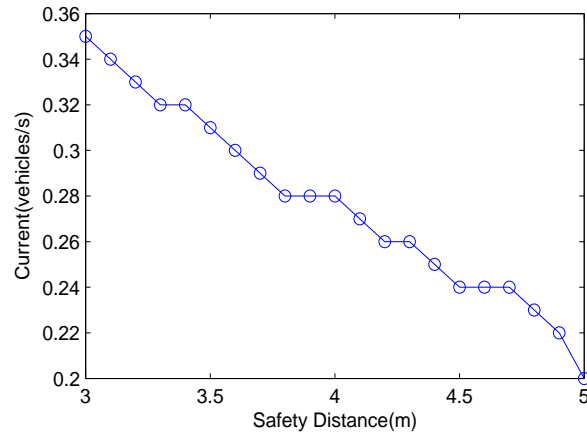


Figure 9 Plot of traffic current of the lane reduction bottleneck under different safety distances for Case 1.

fic flow. Obviously, the number of the vehicles in the sections A and B has been increasing with the appearance of traffic congestion for the reason that the upstream arrival rate is greater the critical value ($R_a=0.13$) making the current of the lane reduction bottleneck achieve its capacity. What's more, it's found that the headway and velocity of the right lane are always greater than that of the left lane in the sections before the merging point, which is consistent with the result of the case in the periodic boundary condition. The distributions of vehicles and traffic states in the sections A and B are determined by the upstream arrival rate and the capacity of bottleneck. The level of the traffic jam in the section A is higher than that in the section B.

We investigated the dependence of traffic current at lane reduction bottleneck on the safety distance for Case 1. Fig. 9 shows the relationship between the saturated current of the lane reduction bottleneck and the safety distance at sufficiently large time with the downstream departure rate $R_d=0.35$ and the upstream arrival rate $R_a=0.35$, where the safety distance increases from 3 to 5 meters. It can be found that the saturated current decreases with the increase of safety distance when the upstream arrival rate and the downstream departure rate are high. Large value of the safety distance in optimal velocity function denotes bad acceleration performance of a vehicle. In real traffic, some oversize vehicles have worse acceleration performance than small cars. Above result of investigation shows that oversize vehicle being prohibited from entering should be advised for the lane reduction bottleneck with high upstream arrival rate to obtain a satisfied traffic current of the bottleneck.

The dependence of traffic current at lane reduction bottleneck on length of the slowdown section B is derived for Case 1. Fig.10 illustrates the relationship between the sat-

urated current of the lane reduce bottleneck and the length of the slowdown section B at sufficiently large time with the downstream departure rate $R_d=0.35$ and the upstream arrival rate $R_a=0.35$, where the length of the section B increases from 50 to 300 meters. Obviously, it can be found that the number of vehicles passing the lane reduction bottleneck during unit time will not changes by varying the length of slowdown section, which means that the saturated current at the lane reduction bottleneck is independent of the length of the slowdown section. It is a very important conclusion for traffic designer to select a proper length of the speed-limited area before the merging points at the lane reduction bottleneck for other rational factors rather than the length of the speed-limited zone.

We simulate the dependence of traffic current of lane reduction bottleneck on maximum speed of the slowdown section B for Case 1. Fig. 11 illustrates the relationship between the saturated current and the maximum speed of the slowdown section B at sufficiently large time with the downstream departure rate $R_d=0.35$ and the upstream arrival rate $R_a=0.35$, where the maximum speed of slowdown section changes from 0.5 to 2.0 m/s. It can be found from Fig.10 that the saturated current at bottleneck increases with the increase of the maximum speed of slowdown section, which means that the number of vehicles passing the merging point M within a unit time is greatly affected by the maximum speed of the speed-limited area. This factor should be considered when the speed-limited area is required to be arranged before the merging points at the lane reduction bottleneck for other necessary factors. It is recommended that the maximum speed of the speed-limited zone is not too low.

Next, we simulate the traffic flow for Case 2 in which the downstream department rate R_d is less than the capacity of the lane reduction bottleneck. Namely, the num-

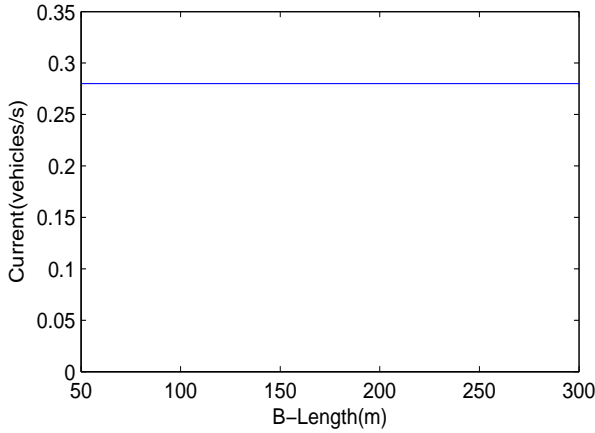


Figure 10 Plot of the saturated current of the lane reduction bottleneck under different length of the slowdown section B.

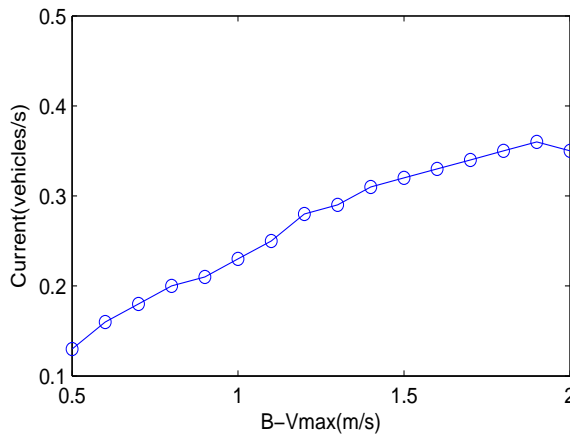


Figure 11 Plot of the saturated current of the lane reduction bottleneck under different maximum speed of the slowdown section B.

ber of vehicles departing from the right end of the section C is less than that passing through the bottleneck in the same time period. Figs. 12 and 13 show the distributions of headway and velocity of vehicles in the road system obtained at sufficiently large time for the downstream departure rate $R_d=0.12$ and the upstream arrival rate $R_a=0.35$. The upstream arrival rate is great enough to allow the current of the lane reduction bottleneck to saturate according to the aforementioned analysis in Fig.5. Apparently, one can observe from Fig.12 and 13 that the vehicles in the section C travel with the same headway and velocity, which are lower than that in Figs. 7 and 8. Similarly, there are two other characteristics we can also notice from the two fig-

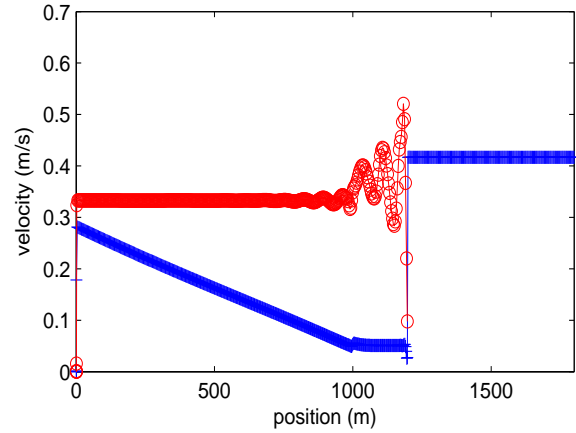


Figure 12 Snapshot of velocity against position on the whole road at the downstream departure rates 0.12(vehicles/s), where the red line with open circles and blue line with plus signs represent the velocity profiles of the right and left lines respectively.

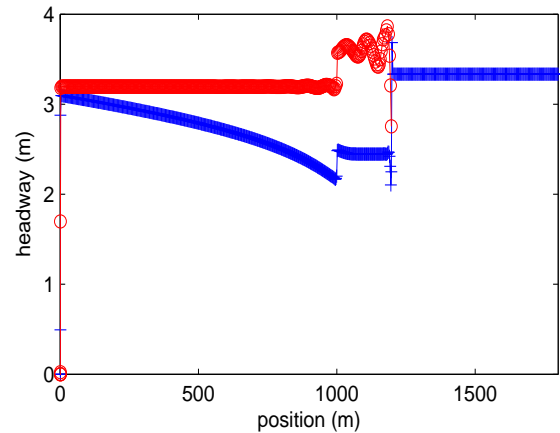


Figure 13 Snapshot of headway against position on the whole road at the downstream departure rates 0.12 (vehicles/s), where the red line with open circles and blue line with plus signs represent the headway profiles of the right and left lines respectively.

ures. one is that the vehicle enters into the section B from the section A with a higher velocity than that in the section A. the other is that the velocities of vehicles on the right lane are higher than that on the left lane in both sections A and B, which is consistent with our observation in the simulation for Case 1. Therefore, this phenomenon appears in the simulations for Case 1 and 2, regardless of what the downstream departure rate. In Ref. [30], two different vehicle types, which are fast vehicle and slow vehicle, are chosen to perform the simulation at the lane reduction bot-

tleneck under the periodic boundary condition. Zhang et.al concluded that the reason that velocities of the vehicles on the right lane are much higher than that on the left lane in the both sections B and A is because the fast vehicles always tend to move on the right lane for the asymmetric lane changing behaviors in the section B [30]. However, all the vehicles in our simulation have the same traffic operating performance with a same optimal velocity function. We also find this unique traffic characteristic. Therefore, it can be concluded that the traffic characteristic that the vehicles are faster on the right lane in both sections B and A is caused by the lane reduction bottleneck and the asymmetric lane changing behaviors in section B instead of the distinguishing of the fast vehicle and slow vehicle.

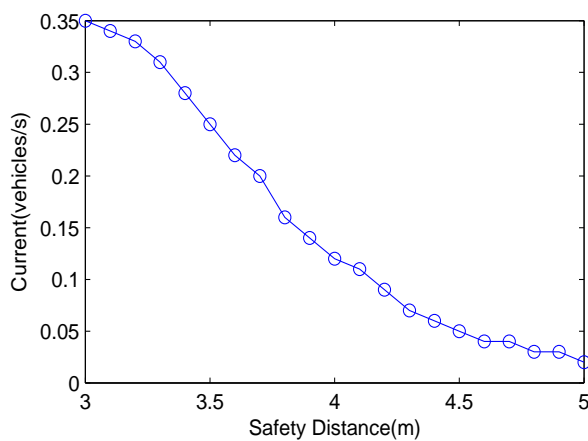


Figure 14 Plot of the traffic current of the lane reduction bottleneck under different safety distances.

We also explore the dependence of traffic current at lane reduction bottleneck on the safety distance for Case 2. Fig.14 indicates the plot of the traffic current at bottleneck under different safety distances at sufficiently large time with the downstream departure rate $R_d=0.12$ and the upstream arrival rate $R_a=0.35$, where the safety distance ranges from 3m to 5m. From Fig. 6, we have known that the traffic current of the lane reduction bottleneck cannot saturate and is limited by the downstream traffic flow when the downstream department rate R_d less than the capacity of the bottleneck. A queue will be formed in the section C and will move left across the merging point M as the time evolution. Nevertheless, from the Fig.14, one can obtain that the effect trend of the safety distance on the saturated current of bottleneck for Case 1 as shown in Fig.9, is nearly the same as the effect trend of the safety distance on the traffic current at bottleneck for Case 2, although traffic current of the lane reduction bottleneck cannot saturate for the limitation of low downstream departure rate in Case 2. Therefore, the proposal that oversize vehicle being prohib-

ited from entering the lane reduction bottleneck with high upstream arrival rate is still right for Case 2.

The dependence of traffic current at lane reduction bottleneck on the length of the slowdown section is also investigated for the Case 2. Fig.15 shows the influence of the length of the slowdown section B on the traffic current of the lane reduce bottleneck at sufficiently large time with the downstream departure rate $R_d=0.12$ and the upstream arrival rate $R_a=0.35$, where the length of the slowdown section B increases from 50 to 300 meters. Apparently, one can see from this figure that the traffic current of the lane reduce bottleneck keeps a constant with the length of section B changing from 50 to 300 meters, which means that the traffic current of the lane reduce bottleneck is independent of the length of the slowdown section B, which is agreement with the result we obtained in Fig.10. The difference between Fig. 10 and 15 is that the constant value (0.12vehicles/s) of traffic current in Fig 15 is smaller than that (0.27vehicles/s) in Fig 10, which is limited by the low downstream departure rate 0.12vehicles/s. It means that the traffic current of the lane reduce bottleneck is not relative to the length of the speed-limited area, regardless of what the downstream departure rate.

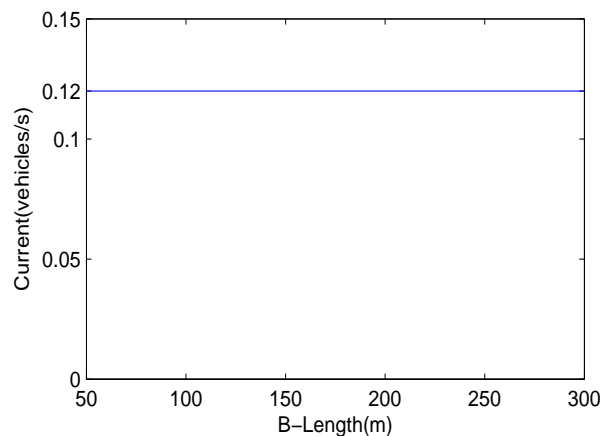


Figure 15 Plot of the traffic current of the lane reduction bottleneck under different lengths of the slowdown section B.

The effect of the traffic current on the maximum speed in the slowdown section B is investigated for Case 2. Fig. 16 gives the traffic current of the lane reduction bottleneck under different maximum speeds in the slowdown section B at sufficiently large time for the downstream departure rate $R_d=0.12$ and the upstream arrival rate $R_a=0.35$, where the maximum speed of slowdown section increases from 0.5 to 2.0 m/s. One can observe that the saturated current of the lane reduction bottleneck is independent of the limited speed of vehicles in slowdown section when the downstream departure rate is low. Namely, the limiting speed

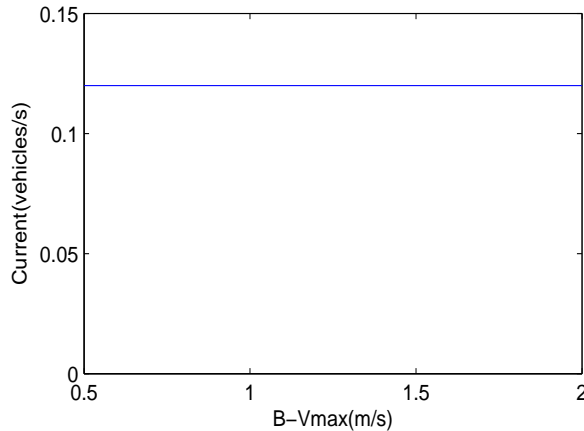


Figure 16 Plot of the traffic current of the lane reduction bottleneck under different maximum speeds of the slowdown section B.

has no effect on the saturated current, which is different from the result in Fig. 11. It means the downstream departure rate is a key determinant of traffic current of the lane reduction bottleneck when downstream departure rate R_d less than the capacity of the bottleneck. Anyway, the proposal that the maximum speed of the speed-limited zone is not too low is also recommended regardless of what the downstream departure rate. At least, it works for the case in which the downstream departure rate is greater than the saturated current of the bottleneck.

4. Conclusion

The study of traffic current of the lane reduction bottleneck under the open boundary condition is interesting and significant for the study to the actual traffic system. In this paper, we have numerically explored traffic current of the lane reduction bottleneck for two-lane road merging into single-lane road under open boundary condition for different upstream arrival rates and downstream departure rates. We have selected two downstream departure rates to investigate the traffic flow at the lane reduction bottleneck, and investigate the dependence of the traffic current of the bottleneck on safety distance, length and maximum speed of slow down section for two cases: one is the case that the downstream departure rate being greater than the capacity of the bottleneck, the other is the case that the downstream departure rate being smaller than the capacity. Some important results have been addressed as follows:

(1) The traffic current at the bottleneck increases with the increase of the upstream arrival rate with the free downstream traffic flow when the upstream arrival rate is less than a critical value, and the traffic current saturates when the upstream arrival rate is greater than the critical value.

(2) When the upstream arrival rate is greater enough to saturate the lane reduction bottleneck, the traffic current at bottleneck can reach its capacity when the downstream departure rate is higher than the capacity of the lane reduction bottleneck. On the other hand, the traffic current of the bottleneck is limited by the downstream departure rate when the downstream departure rate is lower than its capacity.

(3) When the upstream arrival rate is greater enough to saturate the lane reduction bottleneck, vehicles move faster on the right lane than that on the left lane in sections before the merging point regardless of what the downstream departure rate and vehicle type.

(4) The saturated current at lane reduction bottleneck depends on the safety distance and the maximum speed of the slowdown section when the downstream departure rate is greater than the capacity of the bottleneck, while the traffic current at lane reduction bottleneck depends on the downstream departure rate and the safety distance when the downstream departure rate is less than the capacity of the bottleneck.

Acknowledgement

This work is supported by the Natural Science Foundation of China under Grant No. 61202384, the Fundamental Research Funds for the Central Universities under Grant No. 0800219198, the Natural Science Foundation of Shanghai under Grant No. 12ZR1433900, the National High Technology Research and Development Program of China under Grant No. 2012AA112801, and the Scientific Research and Development Program of China Railway Corporation under Grant No. 2013X016-B.

References

- [1] L. A. Pipes, *J. of .App. Phys.* **41**, 74 (1953).
- [2] M. Bando, K. Hasebe, and A. Nakayama, *Phys. Rev. E* **51**, 1035 (1995).
- [3] D. Helbing, B. Tilch, *Phys. Rev. E* **58**, 133 (1998).
- [4] R. Jiang, Q. S. Wu, and Z. J. Zhu, *Phys. Rev. E* **36**, 405 (2001).
- [5] M. Bando, K. Hasebe, K. Nakanishi, *Phys. Rev. E* **58**, 5429 (1998).
- [6] T. Nagatani, *Physica A* **261**, 599 (1998).
- [7] T. Nagatani, *Physica A* **265**, 297 (1999).
- [8] T. Nagatani, *Phys. Rev. E* **60**, 6395 (1999).
- [9] K. Hasebe, A. Nakayama, and Y. Sugiyama, *Phys. Rev. E* **69**, 017103 (2004).
- [10] K. Hasebe, A. Nakayama, and Y. Sugiyama, *Phys. Rev. E* **68**, 026102 (2003).
- [11] G. B. Whitman, *Proc. R. Soc. London, Ser. A* **428**, 49 (1990).
- [12] W.X. Zhu, *Int. J. Mod. Phys. C* **24**, 1350046 (2013).
- [13] W.X. Zhu, C.H. Zhang, *Phys. A* **392**, 3301 (2013).
- [14] G.H. Peng, X.H. Cai, C.Q. Liu, B.F. Cao, and M.X. Tuo, *Phys. A* **375**, 13973 (2011).

- [15] G.H. Peng , R.J. Cheng, Phys. A **392**, 3563 (2013).
 [16] G.H. Peng , D.H.Sun, Chin. Phys. B **18**, 5420 (2009).
 [17] H. X. Ge, S. Q. Dai, L. Y. Dong, and Y. Xue, Phys. Rev. E **70**, 066134 (2004).
 [18] H. X. Ge, S. Q. Dai, Y. Xue, and L. Y. Dong, Phys. Rev. E **71**, 066119 (2005).
 [19] H.X. Ge, R.J Cheng, and Z.P. Li, Phys. A **387**, 5239 (2008).
 [20] D. Helbing, Rev. Modern Phys. **73**, 1067 (2001).
 [21] D. Chowdhury, L. Santen, A. Schadscheider, Phys. Rep. **329**, 199 (2000).
 [22] B.S. Kerner, The Physics of Traffic, Springer, Heidelberg, (2004).
 [23] W. Shi, Y.L. Mo, Y. Xue, in: ICNM-V, Peoples R China, Shanghai, (2007).
 [24] T. Q. Tang, H. J. Huang, Y. Xue, Acta. Phys.sin. **55**, 4026 (2006).
 [25] T. Q. Tang, H. J. Huang, S. G. Zhao, and G. Xu, Mod. Phys. B **23**, 743 (2009).
 [26] T. Q. Tang, C. Y. Li, H. J. Huang, and H. Y. Shang, Theor. Phys. **54**, 1151 (2010).
 [27] B. Jia, R. Jiang, Q.S.Wu, Int. J. Mod. Phys. C **14**, 1295 (2003).
 [28] B. Jia, R. Jiang, Q.S.Wu, Phys. Rev. E **69**, 056105 (2004).
 [29] P. Sheng, S.L. Zhao, J.F.Wang, H. Zuo, Acta Phys. Sin. **59**, 3831 (2010)(in Chinese).
 [30] J. Zhang, X.L. Li, R. Wang, X.S. Sun, X.C. Cui, Phys. A **391**, 2381 (2012).
 [31] S. Kurata, T. Nagatani, Physica A **318**, 537 (2003).
 [32] H. B. Zhu, L. Lei, S. Q. Dai, Physica A **388**, 2903 (2009).



Zhipeng Li received his Ph.D degree in pattern recognition and intelligent system form Shanghai Jiao Tong University, Shanghai, China, in 2007. Currently, he is a Associate Professor in the department of information and communication in Tongji University, China. He holds

six Chinese patents and has published over 70 papers in refereed journals and conference proceedings. His current research interests include traffic flow modelling, Intelligent transportation system, image processing, and pattern recognition.



Run Zhang obtained the Bachelor Degree of Engineering from Tongji University, Shanghai, China with the major of Communication Engineering in July 2012. He is good at numerical simulation. He has proposed the Dynamic Cooperation car-following model with better traffic stability. And he has published some articles in important magazines. Now he is a master student of Tongji University, China.



Shangzhi Xu received his Ph.D degree in signal and information processing from university of science and technology of China, Hefei, china, in 2006. Currently, he is a lecturer in the department of information and communication in Tongji University, China. He has published over 10 papers in

refereed journals and conference proceedings. His current research interests include image processing, pattern recognition, video Surveillance System, and Intelligent transportation system.



Yeqing Qian received her Ph.D degree in Communication and Information system from Huazhong University of Science and Technology, Wuhan, China, in 2004. From 2010 to 2011, She was as a visiting scholar at the universtiy of

Ruhr-Universitaet Bochum, Germany. Currently, She is a researcher in the infomation Processing and ITS Lab of Tongji University. She is a researcher in the infomation Processing and ITS Lab of Tongji University. She has published over 20 papers in refereed journals and conference proceedings. Her current research interests include Intelligent transportation system, Wireless Communication etc.